Active Site Properties of the 3C Proteinase from Hepatitis A Virus (a Hybrid Cysteine/Serine Protease) Probed by Raman Spectroscopy†

Deendayal Dinakarpandian,‡ Bhami Shenoy,‡ Marianne Pusztai-Carey,‡ Bruce A. Malcolm,§ and Paul R. Carey*,‡

Department of Biochemistry, Case Western Reserve University, 10900 Euclid Avenue, Cleveland, Ohio 44106, and Department of Biochemistry, University of Alberta, Edmonton, Alberta, Canada T6G 2H7

Received December 27, 1996; Revised Manuscript Received February 20, 1997⊗

ABSTRACT: Although the HAV 3C proteinase is a cysteine protease, it displays an active site configuration which resembles mammalian serine proteases and is structurally distinct from the papain superfamily of thiol proteases. Given the interesting serine/cysteine protease hybrid nature of HAV 3C, we have probed its active site properties via the Raman spectra of the acyl enzyme, 5-methylthiophene acryloyl HAV 3C, using the C24S variant of the enzyme to obtain stoichiometric acylation. The Raman difference spectral data show that the major population of the acyl groups in the active site experiences electron polarization intermediate between that in the papain superfamily and that in a nonpolarizing site. This is evidenced by the values of the acyl group ethylenic stretching frequency which occur near 1602 cm^{-1} in a nonpolarizing environment, at 1588 cm^{-1} when bound to HAV 3C (C24S), and at 1579 cm^{-1} in acyl papains. The value of the electronic absorption maximum for the HAV 3C (C24S) acyl enzyme and the deacylation rate constant fit the correlation developed for the papain superfamily, suggesting that for HAV 3C too, polarizing forces in the active site can contribute to rate acceleration via transition state stabilization. The major population in the active site is *s-cis* about the acyl group's C1−C2 bond, but there is a second population that is *s-trans*, and this secondary population is not polarized. The two populations are evidenced by the presence of two sets of marker bands for *s-cis* and *s-trans* in the Raman spectra, which occur principally in the C═C stretching region near 1600 cm^{-1}, in the C−C stretching region near 1100 cm^{-1}, and near 560 cm^{-1}. The positions of the acyl carbonyl features in the Raman spectra point to hydrogen-bonding strengths of 20−25 kJ mol^{-1} between the C═O and H-bonding donors in the active site. The 5-methylthiophene acryloyl HAV 3C (C24S) is a relatively unreactive acyl enzyme, deacylating with a pK_a of 7.1 and a rate constant of 0.000 31 s^{-1} at pH 9. Unlike most other cysteine or serine protease acyl enzymes characterized by Raman spectroscopy, no changes in the Raman spectrum could be detected with changes in pH.

The picornaviridae are a family of small, closely related RNA viruses responsible for a variety of human and animal pathologies; the most famous and well-studied member of the family is the causative agent of poliomyelitis. In addition, the family includes rhinovirus, the etiologic agent for the majority of common colds; hepatitis A virus (HAV), which produces a usually benign form of hepatitis; and foot and mouth disease virus, a highly contagious livestock pathogen. The viral 3C gene products are a novel group of cysteine proteinases responsible for the bulk of the polyprotein processing (Kräusslich & Wimmer, 1988). Although cysteine proteinases, they display active site configurations like those of the mammalian serine proteinases (Allaire *et al.,* 1994; Matthews *et al.,* 1994) and are structurally distinct from the papain family of thiol enzymes (Malcolm, 1995). The crystal structure of the 3C proteinases from hepatitis A virus and rhinovirus 14 have shown that these enzymes adopt a two-domain β-barrel fold similar to that of chymotrypsin. The critical active site geometries of the nucleophilic cysteine side chain, as well as that of the histidine general base, are virtually superimposable with the equivalent residues, serine 195 and histidine 57, of chymotrypsin (Bergmann *et al.,* 1997).

The HAV 3C proteinase, unlike the 3C enzyme of rhinovirus, does, however, exhibit one departure from the conformation of the active site of the serine proteinases. The side chain of Asp 84 (analogous to Asp 102 of chymotrypsin) points away from the general base, His 44, and is clearly involved in interactions with Lys 202 and Asp 158 (Allaire *et al.,* 1994; Bergmann *et al.,* 1997). Thus, unlike the rhinovirus enzyme (Matthews *et al.*, 1994), for HAV there does not appear to be a 'third member' of the expected catalytic triad. The absence of any carboxylic acid, suitably positioned in the structure of the HAV 3C, suggests that either an alternative mechanism is at work in this particular 3C proteinase or the thiolate−imidazolium system is sufficient for catalysis (Allaire *et al.,* 1994), as generally accepted for the papain family of thiol proteinases (Drenth *et al.,* 1976).

The intriguing hybrid nature of HAV 3C, containing elements of both conventional serine and cysteine proteases, and the mechanistic questions which derive from this have prompted us to use Raman spectroscopy to probe the chemistry of bound acyl groups. In a series of studies with serine proteases, we were able to use Raman data to

† This work was supported by NIH Grant GM-54072-01 (to P.R.C.) and MRC of Canada Grant DG-N013 (to B.A.M.).

* To whom correspondence should be addressed. E-mail, carey@biochemistry.cwru.edu; Fax, 216-368-4544; Tel, 216-368-0031.

‡ Case Western Reserve University.

§ University of Alberta.

⊗ Abstract published in *Advance ACS Abstracts,* April 1, 1997.

S0006-2960(96)03148-0 CCC: $14.00

characterize the effect of activating the charge relay system on the acyl group of an enzyme intermediate, by going to pH 8−10 (Phelps *et al.*, 1981; Tonge & Carey, 1989; Carey & Tonge, 1995). Moreover, features due to the acyl C═O group could be detected and provided a measure of both bond length and strength of hydrogen bonding to the C═O linkage. A strong correlation was observed between the C═O bond length and the logarithm of the deacylation rate constant (Tonge & Carey, 1992; Carey & Tonge, 1995). The situation for cysteine proteases is quite different. Recent studies (Doran *et al.*, 1996; Doran & Carey, 1996) have shown that effects in the Raman and electronic absorption spectra are dominated by electron polarization. Active site forces, for which an α-helix dipole is a major candidate, set up a dipole along the long axis of the chromophoric acyl group used in the Raman studies, typically a thiophene acryloyl or cinnamoyl derivative. Strong electrical forces in the active site have been proposed to accelerate catalysis by stabilizing charge buildup in the transition state (Doran & Carey, 1996). For the acyl enzyme 5-methylthiophene acryloyl HAV 3C, we now find that, as for cysteine proteases in the papain superfamily, the acyl group binds mostly as the *s-cis* conformer about the acyl group C1−C2 bond. However, this population shows evidence of only modest polarization in its π-electron chain.

Initial trials at forming 5-methylthiophene acryloyl HAV 3C revealed that more than one acyl group per enzyme molecule was binding, and the absorption spectra indicated that more than one cysteine was being acylated. This problem was overcome by using the C24S variant of the protein. This is kinetically indistinguishable from the wild-type and acylates with stoichiometric amounts of 5-methylthiophene acryloyl. The acyl enzyme, using the C24S variant, then deacylates fully with simple first-order kinetics.

MATERIALS AND METHODS

Proteinase Production and Purification. Recombinant C24S HAV 3C proteinase (a mutant in which the nonessential surface cysteine was replaced with serine and which exhibits identical catalytical parameters to wild-type enzyme, unpublished results) was expressed in *Escherichia coli* and purified as reported previously (Malcolm *et al.*, 1992). Purity of the enzyme samples was greater than 90% as determined by SDS−PAGE analysis (data not shown). Proteinase concentrations were determined spectrophotometrically, 1.2 mg/mL being equivalent to a unit of optical density.

Synthesis of Substrates. The syntheses of 5-methylthiophene acryloyl imidazolide and its ^{13}C═O and C═^{13}C−C═O isotopomers were performed as described in Tonge *et al.* (1991). The corresponding ethyl thiolesters were prepared by adding 25 mg of the imidazolide to 1 mL of ethanethiol and stirring overnight. Potassium phosphate (300 mL, 50 mM), pH 7.0, was added, followed by extracting twice with 40 mL of methylene chloride. The extract was evaporated under vacuum and the residue purified by HPLC on a supercosil LC-SI column.

Preparation of Acyl Enzyme. Acyl HAV 3C proteinase was prepared using 5-methylthiophene acryloyl imidazolide as follows: The enzyme was acylated by the addition of 5 μL of 5-MTA imidazolide in DMSO to 100 μL of 0.6 mM enzyme solution (final substrate concentration = 2.5 mM). Unreacted substrate was removed after 5 min by low-speed centrifugation in a Sephadex G-25 column (1 mL) previously equilibrated with 0.1 M potassium phosphate buffer, pH 6.5. The acyl enzyme was passed through a 0.45 μm filter prior to obtaining Raman data.

Deacylation Kinetics. For kinetics of deacylation, the enzyme prepared at pH 6.5 was passed through a column containing one of various buffer systems and the deacylation rate was recorded at λ_{max}, 365 nm, using a Shimadzu UV-2101PC spectrophotometer. Rate constants were calculated using "Grafit", the data being fitted to an equation for single exponential decay with offset.

Raman Instrumentation. The Raman spectrometer is described in Kim *et al.* (1993), and the conditions for data acquisition are given in the figure captions. Peak positions were calibrated using cyclohexanone as a standard and the program Spectracalc (Galactic Industries, New Hampshire); they are believed to be accurate to ± 1 cm^{-1} for well-resolved features.

Molecular Modeling. Molecular modeling for the 5-methylthiophene acryloyl ethyl thiolester was performed on a Silicon Graphics Indigo2 workstation using the InsightII interface and Discover software from Biosym/Molecular Simulations. The molecule was built manually and the *s-cis* and *s-trans* isomers about the C−C(═O) bond were minimized until a maximum derivative of 0.001 kcal/mol/Å was achieved in each case.

RESULTS AND DISCUSSION

Evidence That the Acyl Group Binds in Two Conformational States. In the absence of steric constraints, α,β-unsaturated thiolesters exist as a mixture of *s-cis* and *s-trans* isomers about the C1−C2 bond (Fausto *et al.*, 1994; Tonge *et al.*, 1995; O'Connor *et al.*, 1995; Doran & Carey, 1996):

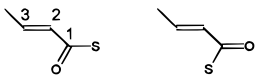

s-cis *s-trans*

The conformational properties of the *s-cis* and *s-trans* conformers of 5-methylthiophene acryloyl ethyl thiolester (5-MTA thiolester) have been investigated using Discover_3 and InsightII software from Biosym, as described in Materials and Methods. The cogent fact to emerge is that both the *s-cis* and *s-trans* thiolesters *in vacuo* can adopt essentially planar conformations differing in energy by less than 3 kcal mol^{-1}. Further, the *s-trans* form is expected to have the larger dipole moment. Taken together, these findings suggest that, with their similar energies, *s-cis* and *s-trans* conformers will coexist in solution and features specific to the *s-trans* conformer will decrease in intensity in solvents of low polarity like CCl_4. The Raman data for 5-MTA thiolester, and its ^{13}C═O and C═^{13}C−C═O isotopomers, in CCl_4, shown in Figure 1, can be discussed with the above conformational findings in mind. The discussion here will focus on those bands which provide insight into the properties of the enzyme-bound 5-MTA moiety.

The spectra in Figure 1 can be understood in terms of an overlay of Raman spectra from the *s-cis* (about C1−C2) and *s-trans* forms of the thiolester. Rotational isomers exist about the S−CH_2CH_3 bond, and possibly about the C3-to-thiophene ring C−C bond, but these have a comparatively minor effect on the Raman spectrum. An important marker band for the *s-cis* and *s-trans* forms is a mode having a high degree of

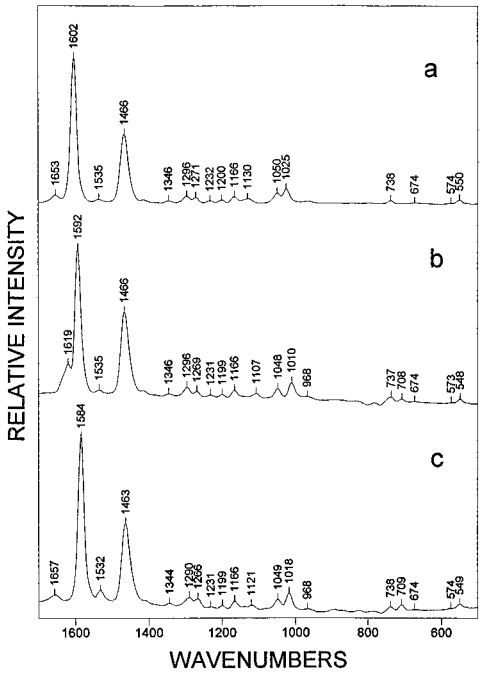

FIGURE 1: Raman spectra of 5-methylthiophene acryloyl ethyl thiolester (a) and its $^{13}C{=}O$ (b) and $C{=}^{13}C{-}C{=}O$ (c) isotopomers, 5−10 mM in CCl_4. Experimental conditions: 488 nm, 350 mW excitation, 5 min spectral accumulation. The displayed data represent the subtraction of solvent from spectrum of thiolester solution.

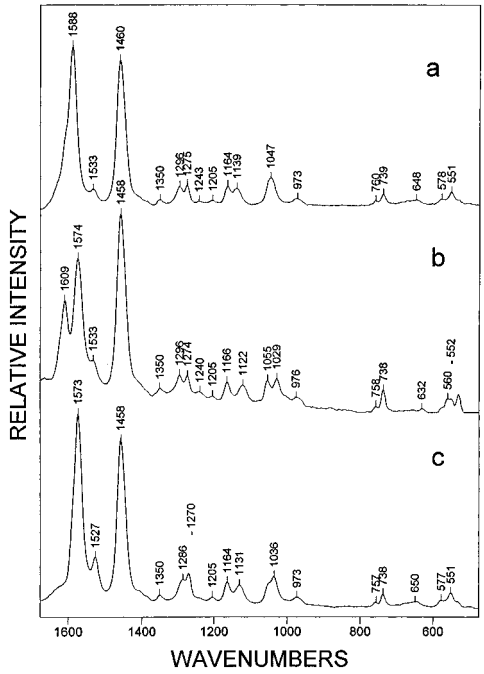

FIGURE 2: Raman difference spectra of the acyl enzymes 5-methylthiophene acryloyl HAV 3C (a) and its $^{13}C{=}O$ (b) and $C{=}^{13}C{-}C{=}O$ (c) isotopomers. The acyl enzymes are 0.5 mM at pH 6.5. Spectral conditions: 488 nm, 350 mW excitation, 20 min spectral accumulation.

C1−C2 stretching character and occurring in the 1000−1150 cm^{-1} region. There is more than one line of evidence to suggest that the band seen in Figure 1a near 1130 cm^{-1} is the C1−C2 feature from the *s-trans* conformer while the band near 1025 cm^{-1} is the corresponding mode for the *s-cis* form. Consistent with their association with C1−C2 stretching motions, both bands move to lower frequency upon $^{13}C{=}O$ or $C{=}^{13}C{-}C{=}O$ substitution. For the α,β-unsaturated thiolester *S*-ethyl thiocrotonate, Fausto *et al.* (1994) used *ab initio* calculations to show that *s-cis* and *s-trans* markers occur near 1035 and 1160 cm^{-1}, respectively. Additionally, Fausto *et al.* (1994) showed that the *s-trans* form has the larger dipole moment and will thus increase in population upon going to solvents with higher dielectric constants. For the $^{13}C{=}O$-labeled 5-MTA thiolester, the ratio of the intensities of the bands near 1010 and 1107 cm^{-1} is 3.3 in CCl_4 (Figure 1b), 2.6 in CH_3CN, and 2.4 in 1:1 CH_3CN:H_2O (data not shown). These solvent data support the assignment of the 1010 cm^{-1} band to the *s-cis* conformer and the 1107 cm^{-1} feature to the corresponding mode from the *s-trans.*

Another example of a *s-cis*/*s-trans* pair in the Raman spectra are the weak bands seen at 550 and 574 cm^{-1} in Figure 1a. The former is a delocalized mode associated with the C−C(=O)−S fragment of the *s-cis* conformer, and the less intense 574 cm^{-1} band is the corresponding mode for *s-trans* (O'Connor *et al.*, 1995). Another point of note, consistent with the observations of Doran and Carey (1996) for acyl cysteine proteases, is that $^{13}C{=}O$ substitution, seen in Figure 1b, has the effect of increasing the relative intensity of the carbonyl stretching mode.

The Raman difference spectra of 5-MTA HAV 3C, for the unlabeled and the $^{13}C{=}O$ and $C{=}^{13}C{-}C{=}O$ isotopomers, are seen in Figure 2 (a more detailed view of the low-frequency region of these spectra appears in Supporting Information). There are three main lines of evidence for the presence of both *s-cis* and *s-trans* conformers in the active site. Firstly, the markers for C1−C2 stretching vibrations from both forms are clearly visible at 1139 cm^{-1} and unresolved with a ring mode near 1047 cm^{-1} in Figure 2a, at 1122 and 1029 cm^{-1} in Figure 2b, and at 1131 and 1036 cm^{-1} in Figure 2c. Secondly, in Figure 2, the *s-cis* marker band is seen at 551 cm^{-1} and its *s-trans* counterpart near 577 cm^{-1}. Thirdly, there is evidence for multiple peaks in the C=C stretching region. There is a shoulder near 1608 cm^{-1} in Figure 2a (which can be resolved by curve fitting, see Supporting Information). In Figure 2b, there is an intense peak at 1574 cm^{-1} and a second weaker band at 1609 cm^{-1}, the curve fitting shown in Figure 3. In Figure 2c, there is a broad feature at 1573 cm^{-1} which resolves into a major peak at 1573 and a minor peak at 1587 cm^{-1} on using curve-fitting techniques (data not shown).

As is usually found for α,β-unsaturated thiolesters (Doran & Carey, 1996), the C=O stretching modes for the acyl carbonyl are very weak in the Raman spectrum and cannot be detected without resorting to curve fitting. Analysis with the Curvefit function of Spectracalc software from Galactic Industries Corporation revealed bands assigned to $\nu_{C=O}$ at 1629, 1620, and 1635 cm^{-1} in Figure 2, panels a, b, and c, respectively. In Figure 3, the underlying peaks in the double bond region of Figure 2b are given. Similar results for Figure 2c are not shown. In Figure 3, the feature near 1620 cm^{-1} is assigned to $\nu_{C=O}$, and by extending the argument made above for a more intense feature from *s-cis*, we assign the 1620 cm^{-1} to $\nu_{C=O}$ from *s-cis*. However, this conclusion must be regarded as tentative, since in the case of the $^{13}C{=}O$-labeled acyl enzyme (Figures 2b and 3) it is likely that significant vibrational coupling occurs between the C=O and C=C stretches. The results for the unlabeled and $^{13}C{=}O$ intermediates demonstrate convincingly, however, that the stretching frequency for the acyl carbonyl occurs near 1630

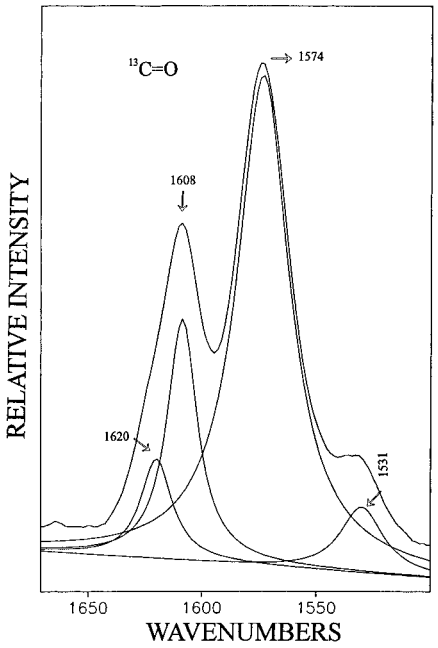

FIGURE 3: Curve fitting of the double bond spectral region for the Raman difference spectrum of 5-methylthiophene acryloyl HAV 3C labeled with ^{13}C═O. Spectra obtained as outlined in Figure 2.

cm^{-1}. This value is about 23 cm^{-1} less than that for $\nu_{C=O}$ for 5-methylthiophene acryloyl ethyl thiolester in the inert solvent CCl_4 (Figure 1). This downshift is likely the result of specific (to the oxyanion hole) or nonspecific (to water molecules or other donors) hydrogen bonding in the active site. By FTIR measurements on model compounds, it is possible to estimate the enthalpy of a hydrogen-bonding interaction that gives rise to an observed shift in carbonyl frequency. The relationship is that each 1 cm^{-1} downshift in $\nu_{C=O}$ corresponds to an increase in hydrogen bond enthalpy of approximately 1 kJ mol^{-1} [for α,β-unsaturated esters, Tonge *et al.*, (1996); for α,β-unsaturated thiolesters, Clarkson and Carey (unpublished work)]. Thus, the acyl carbonyl in the active site of HAV 3C is experiencing a polarizing force equivalent to that caused by a hydrogen bond of about 23 kJ mol^{-1}. This is a fairly modest interaction such as that would result from 1−2 medium strength hydrogen-bonding interactions with water molecules if the model thiolester were in an aqueous environment.

In the low-wavenumber region of the Raman spectra in Figure 2, peaks from laser plasma lines appear at 738 cm^{-1} (Figure 2a−c) and at 531 and 560 cm^{-1} in Figure 2b. Peaks appear from a delocalized mode associated with the C−C(═O)−S fragment, near 551 cm^{-1} for *s-cis* and 578 cm^{-1} for *s-trans*. Several unresolved peaks occur near 650 cm^{-1}, and these are assigned to modes associated with the C−S [from C(═O)−S] stretches. Multiple peaks are expected due to rotational isomerism about S−C as well as C1−C2. Support for our assignment comes from comparing Figure 2, panels a and b where the most intense feature at 648 cm^{-1} shifts down to 632 cm^{-1} upon ^{13}C═O substitution. The feature near 760 cm^{-1} may have a contribution from S−C (cysteine) stretch. (Note that a "magnified" view of the low-wavenumber region spectra is given in Supporting Information).

The π-Electrons in the Bound s-Cis Conformer Are Polarized. The degree of electron polarization in the bound acyl group's π-electrons can be discussed using the values

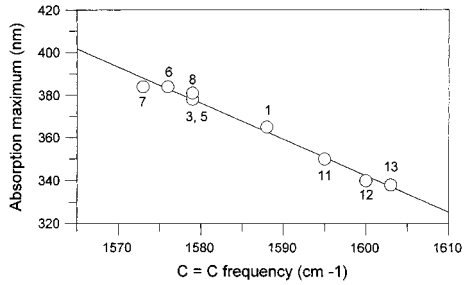

FIGURE 4: Demonstration that the values for *s-cis* 5-methylthiophene acryloyl (5-MTA) HAV 3C fit the correlation of λ_{max} vs $\nu_{C=C}$ established for the papain superfamily acyl enzymes and the thiolester model compound in various solvents. Compound numbering: 1, 5-MTA-HAV 3C; 3, 5-MTA-cathepsin B; 5, 5-MTA-papain; 6, Phe 5-MTA-cathepsin B; 7, Phe 5-MTA-papain; 8, 5-MTA-cathepsin L; 11, 5-MTA-SC_2H_5 (in H_2O); 12, 5-MTA-SC_2H_5 (in CH_3CN); 13, 5-MTA-SC_2H_5 (in CCl_4).

of the ethylenic stretching frequency in the Raman spectrum, $\nu_{C=C}$, and the value of the electronic absorption maximum, λ_{max} (Doran & Carey, 1996; Carey & Storer, 1984; MacClement *et al.*, 1981). Electron polarization occurs as a result of active site forces setting up a permanent dipole in the acyl group:

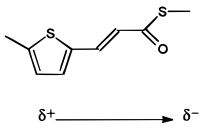

An alternate way to express this is to say that, in the polarized acyl group, canonical (resonance) forms such as II make a larger contribution to the overall structure compared to the case when little or no polarization exists. For the isotopically

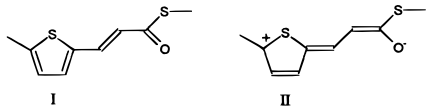

unlabeled acyl-enzyme, the contributions of the ethylenic stretching frequencies from *s-cis* and *s-trans* conformers to the overall profile occur at 1587 and 1608 cm^{-1}, respectively (curve-fitted spectra are seen in Supporting Information). The Raman peak positions for $\nu_{C=C}$ for 5-MTA thiolester are given in Doran and Carey (1996). For the thiolester in CCl_4, CH_3CN, and H_2O, the values are 1603, 1600, and 1595 cm^{-1}, respectively, and represent, essentially, the values for the *s-cis* conformer in the various solvents. In the FTIR spectrum of the model thiolester in CCl_4, the $\nu_{C=C}$ peak for *s-trans* can be seen near 1614 cm^{-1} (data not shown); thus, the weak $\nu_{C=C}$ peak we are observing for *s-trans* in the acyl enzyme is shifted down by only 6 cm^{-1} from that of the model. This is a very weak polarizing effect (Doran & Carey, 1996) and could be due to, for example, hydrogen bonding at the acyl C═O moiety. In contrast, the appearance of $\nu_{C=C}$ for the *s-cis* form at 1587 cm^{-1} is evidence for stronger polarization since it occurs 8−16 cm^{-1} below the values quoted for the model in various solvents. As can be seen in Figure 4, the values for $\nu_{C=C}$ and λ_{max}, for *s-cis*, fit the plot developed for the model thiolester and for acyl enzymes using members of the papain superfamily. The values for 5-MTA HAV 3C (Figure 4) are intermediate between the numbers for strong electron polarization encountered for the papain superfamily

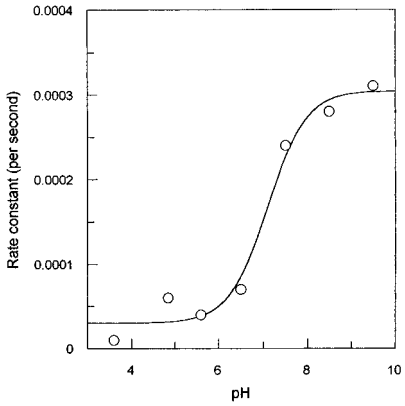

FIGURE 5: Deacylation of 5-MTA-HAV 3C as a function of pH. The rate constants were measured as described under Materials and Methods at various pH values for 5-MTA-HAV 3C and the pK_a was calculated using the program Grafit for single pK_a determination.

and the case of essentially zero polarization seen for the model compound in CCl_4.

In summary, the Raman spectra in the double-bond region are dominated by contributions from the *s-cis* form of the bound acyl group which undergoes "intermediate" polarization by active site forces. Minor contributions can be observed from the *s-trans* population, which experiences very little polarization. Similarly, in the absorption spectrum *s-cis* makes the dominant contribution to the absorption profile with a λ_{max} at 365 nm. The *s-trans* population likely has an absorption maximum on the high-energy side of 365 nm, which is not resolved in the experimental absorption spectrum.

Attempts were made to rationalize the polarization of the 5-MTA and the apparent preference of the HAV 3C enzyme for the *s-cis* isomer. Models of both the *cis* and *trans* 5-MTA acyl HAV 3C were constructed based on the refined structure of the C24S active mutant (Bergmann *et al*., 1997), maintaining optimal geometry between the carbonyl oxygen and the oxyanion hole. From these models it was apparent that the active site would accommodate many different orientations and conformations of the 5-MTA moiety without radically distorting the interactions between the oxyanion hole and the carbonyl oxygen of 5-MTA. The partial polarization of the chromophore and the apparent preference for the *s-cis* isomer were consequently difficult to rationalize and will require additional structural studies before these phenomena can be explained.

Acyl-Enzyme Reactivity. The rate constant for deacylation, as a function of pH, is plotted in Figure 5. Deacylation occurs with a pK_a of 7.1, which is close to the value observed in serine proteases, e.g., 5-MTA chymotrypsin has a pK_a of 7.5 (Tonge & Carey, 1989), but removed from pK_as for similar acyl cysteine proteases, e.g., 5-MTA papain has a pK_a for deacylation of 4.9. The rate constant, k_3, varies from 0.000 01 s^{-1} at low pH to 0.000 31 s^{-1} at high pH. These values are at the low end of the range reported for acyl enzymes from the papain superfamily (Doran *et al.*, 1996) and are 2−3 orders of magnitude less than that for 5-MTA-chymotrypsin (Tonge & Carey, 1989). The k_{cat} for a peptide substrate for HAV 3C is on the order of 1 s^{-1} (Malcolm *et al*., 1992); thus, 5-MTA HAV 3C is comparatively unreactive and this reflects the nonspecific nature of the acyl group and the likelihood that, in either its *s-cis* or *s-trans* conformers in the active site, it is poorly positioned with respect to the deacylation apparatus. This conclusion is reinforced by the observation that, unlike other serine or cysteine-based acyl proteases, changes in the Raman spectrum with variation in pH could not be detected. This implies that the acyl group does not experience the change in protonation state of His 44, for example.

It is interesting to note that the values for the carbonyl stretching frequency, for the $^{13}C{=}O$ isotopomer, and log k_3 fit closely the linear relationship found for these values for eight acyl cysteine proteases from the papain superfamily [see Figure 5 in Doran and Carey (1996)]. As outlined in the work of Doran and Carey (1996), at this time it is not possible to ascribe definitive mechanistic significance to this relationship. However, for the papain superfamily series of acyl enzymes it was proposed that mechanistic insight derives from the observation that a correlation exists between log k_3 and λ_{max} for each acyl enzyme. A red shift in λ_{max} can be explained if the excited electronic state of the bound acyl group has a larger dipole moment than the ground state. As the energy of each state is stabilized by the ambient electric field by an amount proportional to its dipole moment, this is expected to lead to a net reduction in the energy of excitation, i.e., a red shift in the λ_{max} of absorption. Furthermore, it was proposed that, for this substrate, there is a fortuitous similarity between the excited electronic and transition states with respect to the distribution of charge. Therefore, these same electrostatic interactions could accelerate deacylation by stabilizing charge buildup in the transition state for deacylation, resulting in the observed correlation between rate and λ_{max}. This concept appears to apply also for 5-MTA HAV 3C, since the values of λ_{max} and log k_3 fit the correlation shown in Figure 6 of Doran and Carey (1996), with a correlation coefficient of 0.84.

SUPPORTING INFORMATION AVAILABLE

5-Methylthiophene acryloyl HAV 3C and its $^{13}C{=}O$ and $C{=}^{13}C{-}C{=}O$ isotopomers Raman difference spectra and a curve fitting of the double bond spectral region for the Raman difference spectrum of 5-methylthiophene acryloyl HAV 3C (3 pages). Ordering information is given on any current masthead page.

REFERENCES

Allaire, M., Chernaia, M. M., Malcolm, B. A., & James, M. N. G. (1994) *Nature (London) 369*, 72−77.
Bergmann, E. M., Mosimann, S. C., Chernaia, M. M., Malcolm, B. A., & James, M. N. G. (1997) The refined crystal structure of the 3C gene product from Hepatitis A virus: Specific Proteinase Activity and RNA recognition, *J. Virol.* (in press).
Carey, P. R., & Storer, A. C. (1984) *Annu. Rev. Biophys. Bioeng. 13*, 25−49.
Carey, P. R., & Tonge, P. J. (1995) *Acc. Chem. Res. 28*, 8−13.
Doran, J. D., & Carey, P. R. (1996) *Biochemistry 35*, 12495−12502.
Doran, J. D., Tonge, P. J., Mort, J. S., & Carey, P. R. (1996) *Biochemistry 35*, 12487−12494.
Drenth, J., Kalk, K., & Swen, H. M. (1976) *Biochemistry 15*, 3731−3738.
Fausto, R., Tonge, P. J., & Carey, P. R. (1994) *J. Chem. Soc., Faraday Trans. 90*, 3491−3503.
Kim, M., Owen, H., & Carey, P. R. (1993) *Appl. Spectrosc. 47*, 1780−1783.
Kräusslich, H.-G., & Wimmer, E. (1988) *Annu. Rev. Biochem. 57*, 701−754.
Lawson, M. A., & Semler, B. L. (1990) *Curr. Top. Microbiol. Immunol. 161*, 49−80.

MacClement, B. A., Carriere, R. G., Phelps, D. J., & Carey, P. R. (1981) *Biochemistry 20*, 3438−3447.
Malcolm, B. A. (1995) *Protein Sci. 4*, 1439−1445.
Malcolm, B. A., Chin, S. M., Jewell, D. A., Sratton-Thomas, J. R., Thudium, K. B., Ralston, R., Rosenberg, S. (1992) *Biochemistry 31*, 3358−3363.
Matthews, D. A., Smith, W. W., Ferre, R. A., Condon, B., Budahazi, G., Sisson, W., Villafranca, J. E., Janson, C. A., McElroy, H. E., Gribskow, C. L., & Worland, S. (1994) *Cell 77*, 761−771.
Miyashita, K., Kusumi, M., Utsumi, R., Katayama, S., Noda, M., Komano, T., & Satoh, N. (1993) *Protein Eng. 6*, 189−193.
O'Connor, M. J., Dunlap, R. B., Odom, J. D., Hilvert, D., Pusztai-Carey, M., Shenoy, B., & Carey, P. R. (1996) *J. Am. Chem. Soc. 118*, 239−240.
Phelps, D. J., Schneider, H., & Carey, P. R. (1981) *Biochemistry 20*, 3447−3454.
Tonge, P. J., & Carey, P. R. (1989) *Biochemistry 28*, 6701−6709.
Tonge, P. J., & Carey, P. R. (1992) *Biochemistry 31*, 9122−9125.
Tonge, P. J., Pusztai, M., White, A. J., Wharton, C. W., & Carey, P. R. (1991) *Biochemistry 30*, 4790−4795.
Tonge, P. J., Anderson, V. E., Fausto, R., Kim, M., Pusztai-Carey, M., & Carey, P. R. (1995) *Biospectroscopy 1*, 387−394.
Tonge, P. J., Fausto, R., & Carey, P. R. (1996) *J. Mol. Struct. 379*, 135−142.

BI963148X